Bioorganic & Medicinal Chemistry Letters xxx (2014) xxx–xxx

Contents lists available at ScienceDirect

Bioorganic & Medicinal Chemistry Letters

journal homepage: www.elsevier.com/locate/bmcl

Synthesis and antiproliferative activity of imidazo[2,1-*b*][1,3,4]thiadiazole derivatives

Sujeet Kumar [a,1], Vidya Gopalakrishnan [b,1], Mahesh Hegde [b], Vivek Rana [a], Sharad S. Dhepe [a], Sureshbabu A. Ramareddy [a], Alberto Leoni [c], Alessandra Locatelli [c], Rita Morigi [c], Mirella Rambaldi [c], Mrinal Srivastava [b], Sathees C. Raghavan [b], Subhas S. Karki [a,*]

[a] *Department of Pharmaceutical Chemistry, KLE University's College of Pharmacy, Bangalore 560 010, Karnataka, India*
[b] *Department of Biochemistry, Indian Institute of Science, Bangalore 560 012, Karnataka, India*
[c] *Dipartimento di Farmacia e Biotecnologie, Università di Bologna, Via Belmeloro 6, 40126 Bologna, Italy*

ARTICLE INFO

Article history:
Received 29 April 2014
Revised 9 August 2014
Accepted 12 August 2014
Available online xxxx

Keywords:
Antiproliferative agents
Imidazo[2,1-*b*][1,3,4]thiadiazoles
Cell-based screening assay
Hollow fiber assay
Acute toxicity
Apoptosis

ABSTRACT

A series of 2,5,6-substituted imidazo[2,1-*b*][1,3,4]thiadiazole derivatives have been prepared and were tested for antiproliferative activity on cancer cells at the National Cancer Institute. Results showed that molecules with a benzyl group at position 2, exhibited an increase in activity for the introduction of a formyl group at the 5 position. The compound 2-benzyl-5-formyl-6-(4-bromophenyl)imidazo [2,1-*b*][1,3,4]thiadiazole **22** has been chosen for understanding the mechanism of action by various molecular and cellular biology studies. Results obtained from cell cycle evaluation analysis, analysis of mitochondrial membrane potential and Annexin V-FITC by flow cytometric analysis, ROS production and expression of apoptotic and DNA-repair proteins suggested that compound **22** induced cytotoxicity by activating extrinsic pathway of apoptosis, however, without affecting cell cycle progression.

Cancer is a disease of uncontrolled cell growth and is one of the prime diseases to be cured at the present generation.[1] Among different cancers, leukemia, and lymphoma account for 8% of all cancer.

Development of novel small molecule inhibitors against different cancers, particularly leukemia and lymphoma is an area of active investigation.[2] Kinases, a target involved also in chronic myelogenous leukemia, have been widely studied, leading to the development of several inhibitors.[3,4] Besides, novel small molecule inhibitors against DNA repair is also investigated by us and others. Recently, we have shown that small molecule inhibitor, SCR7, can interfere with the binding of Ligase IV to the broken DNA and prevent nonhomologous DNA end joining.[5]

Although there are many drugs currently under trial against cancer and particularly haematological malignancies, only few molecules have emerged as promising drugs. To overcome this, it is important to develop potent anticancer drugs with novel chemical backbones. Gadad et al. in 1999 reported on the antitumor effects of imidazo[2,1-*b*][1,3,4]thiadiazoles[6] and in 2003 Terzioglu et al. reported some hydrazone derivatives of 2,6-dimethyl imidazo [2,1-*b*][1,3,4]thiadiazole-5-carbohydrazide as anticancer agents against ovarian cancer cell line OVCAR.[7] Moreover, a large number of imidazothiadiazole derivatives have been reported to possess diverse pharmacological properties such as antitubercular,[8] antibacterial,[9] antifungal,[10] anticonvulsant, analgesic,[11] antisecretory,[12] anti-inflammatory,[13] cardiotonic,[14] diuretic[15] and herbicidal[16] activities.

Considering the importance of this scaffold, we focused our research on the synthesis of imidazo[2,1-*b*][1,3,4]thiadiazole derivatives endowed with anticancer activity.[17] Among them, compound **4a** (Chart 1) exhibited maximum cytotoxicity by inducing extrinsic pathway of apoptosis without affecting the cell cycle.

On the basis of these results, using **4a** as lead compound, we synthesized a series of analogs in order to investigate their antiproliferative activity. Most of the planned compounds bear the same substituent as compound **4a** at the 2 position (benzyl group), and at the 5 position (formyl group), whereas other derivatives bear different groups such as cyclohexylethyl or ethyl at the 2 position, Br and SCN at the 5 position. Furthermore, the substituent at the *para* position of the 6-phenyl ring was changed. In order to study the SAR, the antiproliferative activity of previously reported compounds was also investigated.

We have synthesized a series of derivatives of imidazo[2,1-*b*] [1,3,4]thiadiazole bearing the above mentioned substituents at 2,

* Corresponding author.
E-mail address: subhasskarki@gmail.com (S.S. Karki).
[1] Equal first authors.

http://dx.doi.org/10.1016/j.bmcl.2014.08.032
0960-894X/

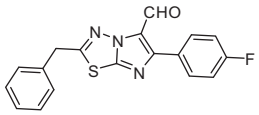

Chart 1. Cytotoxic agent described as **4a** in Ref. [17].

5 and 6 positions. The 2-aralkyl/alkyl/-6-aryl-imidazo[2,1-*b*][1,3,4]thiadiazole derivatives **5**–**12**, reported in Scheme 1, were prepared by reaction of 2-amino-5-substituted-1,3,4-thiadiazoles **1**–**3**, with the appropriate phenacyl bromide (**4**). The compounds **5**–**9** were previously reported in the literature[18,19] and compound **12** reported in literature[20] without spectral data. For the compound **11**, although commercial, we set up a procedure for its synthesis.

The starting 2-amino-5-substituted-1,3,4-thiadiazoles were prepared according to the literature,[21–23] whereas the various phenacyl bromides are commercially available or prepared by bromination of the corresponding ketones in glacial acetic acid. The 2-aralkyl/alkyl/-6-aryl-imidazo[2,1-*b*][1,3,4]thiadiazole derivatives (**5**–**8**, **10** and **11**) were subjected to electrophilic substitution at position 5 with bromine in the presence of sodium acetate in acetic acid to obtain the 5-bromo derivatives **13**–**18** in good yield. The 2-benzyl-6-phenylimidazo[2,1-*b*][1,3,4]thiadiazole-5-carbaldehyde (**19**) was reported in a patent[24] without spectral values. For the aldehydes **20**, **21**, **23** and **24** although commercial, we synthesized by means of the Vilsmeier reaction. Introduction of thiocyanate functional group at the 5 position was carried out by reaction with potassium thiocyanate in glacial acetic acid by drop wise addition of bromine in glacial acetic acid to get **25**–**29** in good yield.

Structures of the synthesized compounds were established on the basis of IR, ^{1}H NMR and mass spectra and CHN data. All synthesized compounds showed absorption bands ranging from 3172 to 3019 cm^{-1} for C—H aromatic stretching, 2999–2825 cm^{-1} for C—H aliphatic stretching. Compounds **19**–**24** showed peaks at 1683–1671 cm^{-1} for C=O stretching. Compounds **25**–**29** showed vibration bands at 2164–2159 cm^{-1} for SCN in their respective IR spectra.

In ^{1}H NMR, the presence of singlet between δ 8.64 and 7.88 ppm for imidazole proton (C_5—H) confirmed the cyclization of 2-amino-5-substituted-1,3,4-thiadiazole **1**–**3** with respective phenacyl bromide. All 5-substituted derivatives showed the absence of C_5—H in their respective spectra confirmed the substitution at 5th position. Compounds **19**–**24** showed a singlet between δ 10.20 and 10.03 ppm for CHO proton. All the compounds showed prominent signals for aromatic protons around δ 8.64–6.94 ppm. Bridge headed methylene proton at C_2 appeared between δ 4.48 and 4.21 ppm for **13**–**16**, **19**–**22**, **25**–**29** derivatives. For the compounds **10**, **17**, and **23** alkyl protons appeared between δ 1.80 and 0.93 ppm. The compounds **12** and **27** showed OCH_3 proton between δ 4.33 and 3.87 ppm. Compounds **11**, **12**, **18** and **24** showed ethyl protons between δ 1.49 and 1.31 ppm for CH_3 as triplet and δ 3.21–3.05 ppm for CH_2 as quartet, respectively.

As a preliminary test, the compounds were tested at a single high concentration (10^{-5} M) in the full NCI 60 cell panel (NCI 60 Cell One-Dose Screen). This panel is organized into subpanels representing leukemia, melanoma and cancers of lung, colon, kidney, ovary, breast, prostate and central nervous system. Only compounds with pre-determined threshold inhibition criteria in a minimum number of cell lines progress to the full 5-concentration assay. These criteria were selected to efficiently capture compounds with anti-proliferative activity based on careful analysis of historical Developmental Therapeutics Program (DTP) screening data. The one-dose data is a mean graph of the percent growth of treated cells (unpublished results).

Compounds **6**, **15**, **21**, **22**, **23**, **25** and **27** were active at a high concentration (10^{-5} M) and therefore entered the 5-concentration test. They were dissolved in DMSO and evaluated using five concentrations at 10-fold dilutions, the highest being 10^{-4} M. Table 1 shows the results obtained, expressed as micromolar concentration at three assay endpoints: the 50% growth inhibitory power (GI_{50}), the cytostatic effect (TGI = Total Growth Inhibition) and

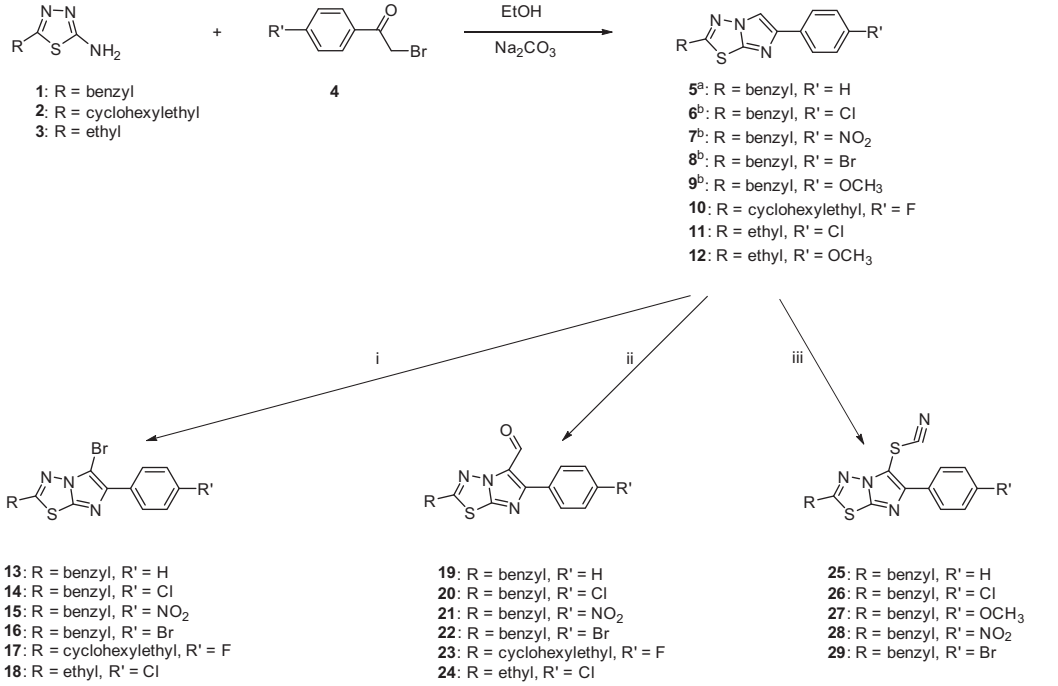

Scheme 1. Synthesis of 2,5,6-substituted imidazo[2,1-*b*][1,3,4]thiadiazole derivatives. [a]Ref. 18; [b]Ref. 19. Reagents and conditions: (i) Br_2, CH_3COOH. (ii) DMF, $POCl_3$, 80–90 °C—Na_2CO_3. (iii) KSCN, Br_2, CH_3COOH.

Table 1
Nine subpanels at five concentrations: growth inhibition, cytostatic and cytotoxic activity (μM) of selected compounds

Compd[a]	Modes	Leukemia	NSCLC	Colon	CNS	Melanoma	Ovarian	Renal	Prostate	Breast	MGMID[b]
6	GI_{50}	2.1	7.6	2.2	5.0	3.7	4.6	2.6	2.9	4.0	3.7
	TGI	23.4	20.9	5.3	13.8	8.9	10.5	5.9	8.1	12.0	11.0
	LC_{50}	95.5	57.5	14.1	34.7	21.9	30.9	15.1	23.4	49.0	31.6
15	GI_{50}	69.2	12.6	52.5	3.4	40.7	6.3	3.7	42.7	17.4	16.2
	TGI	–	56.2	83.2	47.9	–	83.2	64.6	–	79.4	75.9
21	GI_{50}	5.9	2.9	3.1	2.9	3.7	4.1	3.7	3.0	2.8	3.5
	TGI	26.3	45.7	31.6	26.9	42.7	39.8	58.9	50.1	26.3	38.0
	LC_{50}	69.2	95.5	85.1	83.2	–	–	–	–	83.2	91.2
22	GI_{50}	1.41	4.2	2.2	2.2	3.2	4.2	3.2	3.0	3.5	2.9
	TGI	13.5	30.2	10.0	7.4	19.5	41.7	20.0	24.6	28.2	19.5
	LC_{50}	–	95.5	81.3	64.6	81.3	–	93.3	–	–	89.1
23	GI_{50}	10.2	13.2	5.9	7.1	21.9	12.3	14.1	7.4	11.8	11.5
	TGI	70.8	75.9	63.1	67.6	87.1	97.7	93.3	–	61.7	79.4
25	GI_{50}	13.5	6.0	11.2	4.4	20.9	9.8	15.1	15.5	7.4	10.5
	TGI	57.5	75.9	91.2	77.6	85.1	79.4	70.8	40.7	75.9	75.9
	LC_{50}	–	97.7	–	–	–	97.7	95.5	–	–	97.7
27	GI_{50}	3.6	4.6	4.1	3.9	5.8	5.6	7.9	16.2	4.8	5.1
	TGI	72.4	52.5	61.7	55.0	77.6	56.2	70.8	-	60.3	64.6
	LC_{50}	–	83.2	–	–	89.1	–	–	–	–	95.5
Std	GI_{50}	3.2	14.5	10.0	21.4	15.5	18.6	15.9	10.0	16.6	12.6

The GI_{50} and TGI values are reported only when <100 M.
The compound exposure time was 48 h.
Std = Rifamycin SV.
[a] Highest concd tested = 10^{-4} μM.
[b] Mean Graph MIDpoint: average value for all cell lines tested; that is, mean GI_{50}.

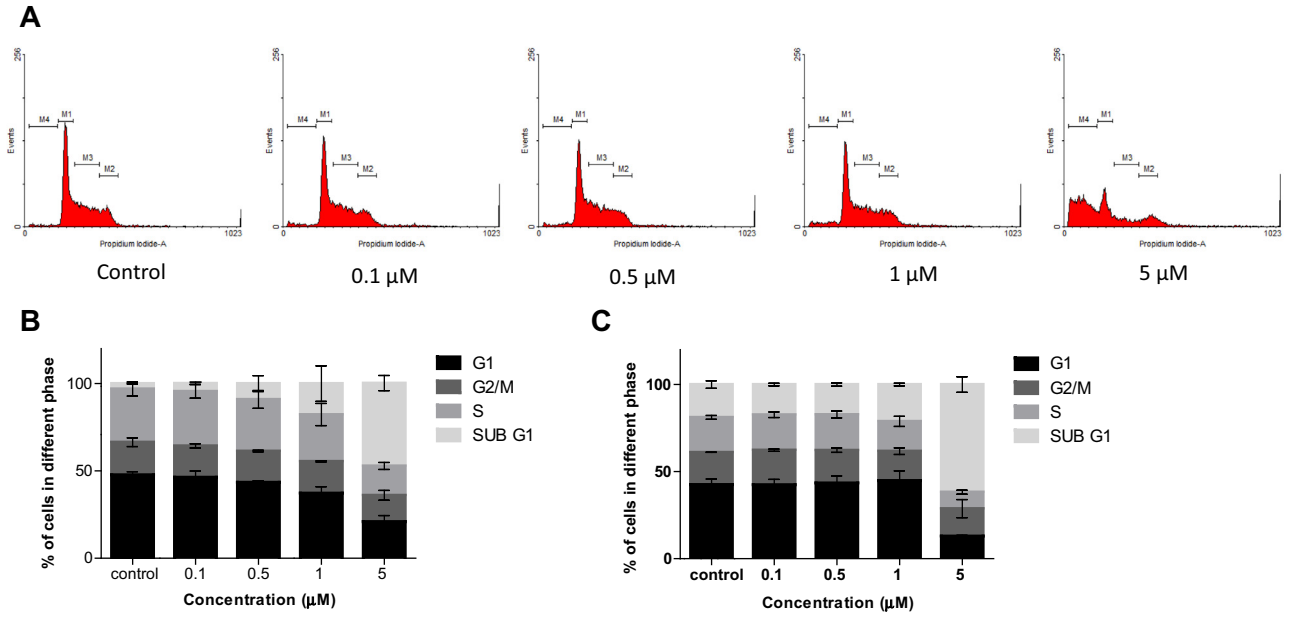

Figure 1. Cell cycle analysis of Reh and Nalm6 cells following **22**-treatment. Reh cells were treated with **22** (0.1, 0.5, 1 and 5 μM) for 48 h, harvested, stained with propidium iodide and subjected to flow cytometry. (A) Histogram obtained after FACS analysis for Reh cells. Histograms show the percentage of cells in the sub G1, G1, S and G2 phases of the cell cycle. In the histogram M1 is G1, M2 is G2, M3 is S and M4 is sub G1 phase (B and C). Bar diagram representing the cell cycle progression of Reh (B) and Nalm6 (C) cells. The data presented is derived from three independent experiments for REH and two independent experiments for Nalm6 and error bars are indicated. For each sample, 10,000 cells were used for sorting.

the cytotoxic effect (LC_{50}). Rifamycin SV has been selected as the reference drug since in the COMPARE analysis (http://dtp.nci.nih.gov/docs/compare/compare.html) showed significant correlation with these compounds. Moreover antitumor effects of Rifamycins on a variety of human cancer-derived cells have been reported.[25] For compounds **6**, **15**, **21** and **25**, the 5-concentration test was repeated and no significant differences were found. For these compounds the data reported in Table 1 are the mean values between the two experiments. Compound **6** was submitted to BEC (Biological Evaluation Committee) for a possible future development.

The tested compounds showed a mean pGI_{50} range between 16.2 and 2.9 μM. The biological activity of the compounds is not correlated with their calculated log*P* (Supplementary Table).

In light of the NCI-60 results, the following considerations may be done: the benzyl substituent at the 2 position, chosen for most of the derivatives synthesized, proved to be very interesting in fact

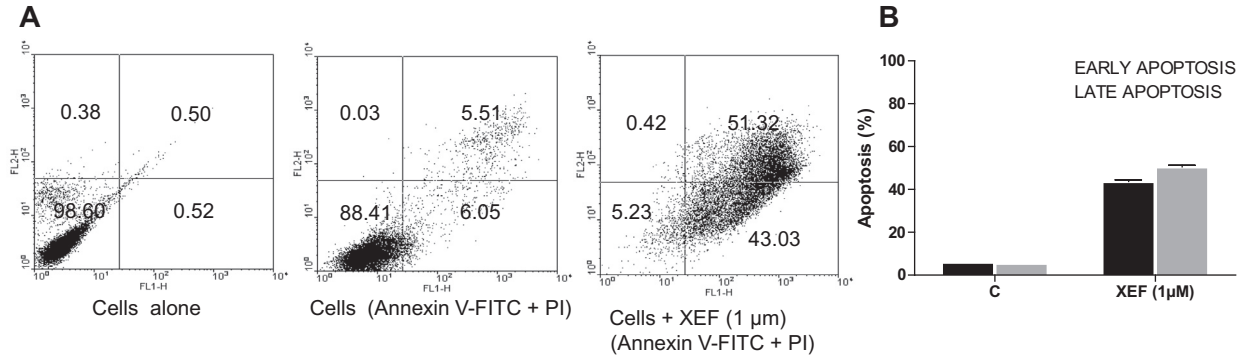

Figure 2. Detection of apoptosis induced by **22** in Reh cells. After **22**-treatment (1 μM) for 48 h, Reh cells were stained with annexin V-FITC and PI, and analyzed by flow cytometry. (A) In each panel, the lower left quadrant shows cells which are negative for both annexin V-FITC and PI, lower right shows annexin V positive cells which are in the early stage of apoptosis, upper left shows only PI positive cells which are dead, and upper right shows both annexin V/PI positive, which are in the stage of late apoptosis or necrosis. The values mentioned in the quadrants show the percentage of early apoptotic cells or late apoptotic cells and necrotic cells in control as well as treated cases. (B) Bar diagram showing percentage of cells in different apoptotic phases.

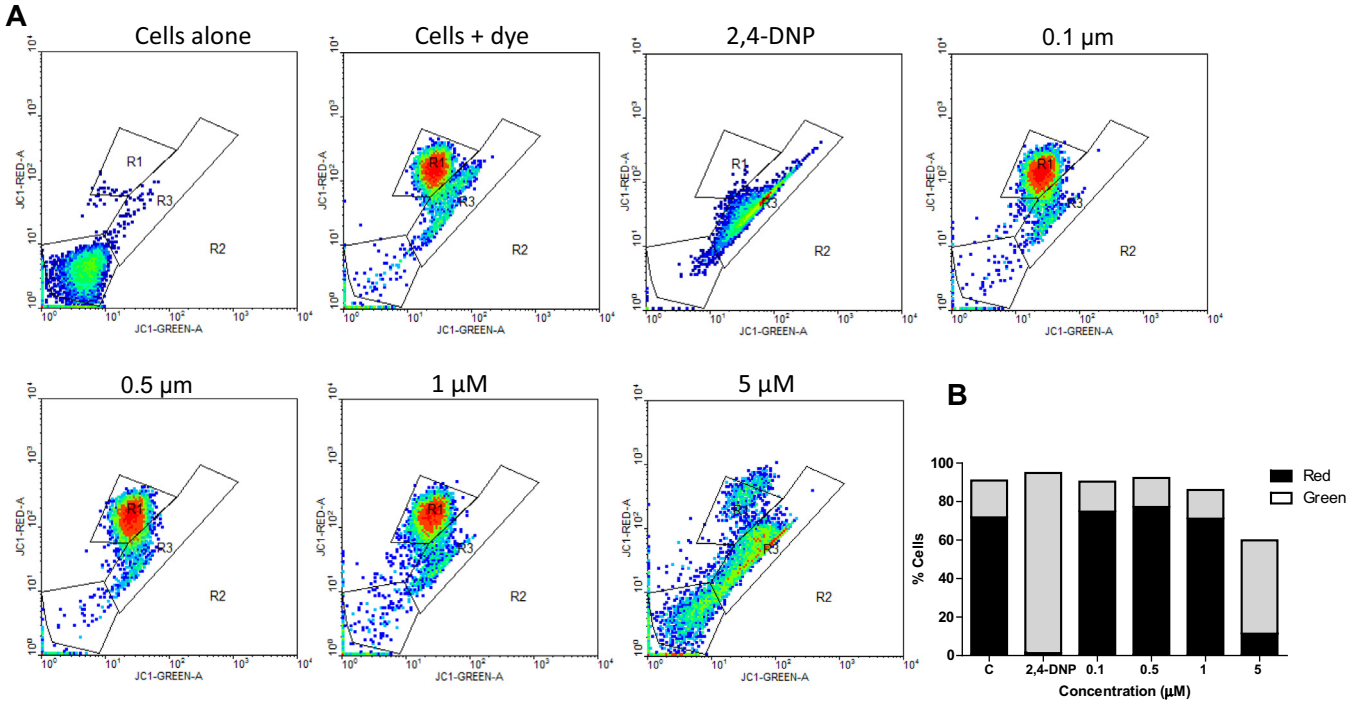

Figure 3. Detection of loss of mitochondrial membrane potential followed by **22**-treatment. Reh cells were treated with **22** (0.1, 0.5, 1 and 5 μM) for 48 h, harvested, stained with JC-1 dye, and analyzed by flow cytometry. 2,4-DNP treated Reh cells were served as positive control. (A) Dot plot representing JC-1 stained cells at different concentration of **22**. (B) Bar diagram showing ratio of red versus green fluorescent cells.

the introduction of an ethyl group gave compounds inactive in the single concentration test and the cyclohexylethyl group was useful only when a formyl group was present at the 5 position (**23**).

As far as the 5 position is concerned, Br is not favorable since among the compounds with this substituent only compound **15** was active (GI_{50} 16.2 μM) whereas there is an increase in activity with the introduction of the SCN group since two compounds entered the 5-concentration screen and compound **27** showed GI_{50} = 5.1 μM with low toxicity (LC_{50} 95.5 μM).

The formyl group gave good results: Besides the aforementioned compound **23**, even the 2-benzyl derivatives **21** and **22** deserve a mention for their high growth inhibitory activity (mean GI_{50} 3.5 and 2.9 μM, respectively) and low toxicity (mean LC_{50} 91.2 and 89.1 μM).

Further studies continued at the NCI where the maximum tolerated dose (MTD) was determined for **6**. It was found to be 400 mg/kg for the compound administered IP in DMSO. In light of this result, BEC decided to submit **6** to the hollow fiber test.[26] The compound was not active enough to warrant further testing.

Effect on growth inhibition of leukemic cells: Based on above results, cytotoxic effects of the most active compounds on leukemic cell lines **6** and **22**, were further investigated. Firstly, leukemic cell lines, Reh (pre B-cell leukemia), K562 (chronic myelogenous leukemia) and Nalm6 (pre B-cell leukemia), were treated with increasing concentrations of compounds **6** (10, 50, 100 and 250 μM) or **22** (0.1, 0.5, 1, 5 and 10 μM) and cell viability was determined by trypan blue assay, after 24, 48 and 72 h of addition of compounds (Fig. S1A and C).[27] The DMSO treated cells served as vehicle control as the compounds were dissolved in DMSO. Interestingly, compound **22** showed a time-dependent inhibition on cell viability in all the three leukemic cell lines, while the effect was less in the case of compound **6** (Fig. S1A and C). The compound

22 exhibited increased cell death at concentrations of 5 μM and above in the cell lines, Reh and Nalm6 (Fig. S1C and D). The growth of control cells and DMSO treated cells were comparable (data not shown). Thus results suggest that **22** induce cytotoxicity in human leukemic cells in a dose- and time-dependent manner. The effect of **6** and **22** on leukemic cells was further verified using MTT assay. In order to do this, cells treated with compounds **6** (10, 50, 100 and 250 μM) or **22** (0.1, 0.5, 1, 5 and 10 μM) were harvested after 48 and 72 h, and subjected to the assay. The results showed that compound **6** was less effective even at higher concentrations in the cell lines tested, while **22** showed significant cytotoxic effect at 5 and 10 μM concentrations (Fig. S1B and D).

Cytotoxic effect of **22** (3 μM) on leukemic cells, Reh, and normal cell 293T (human kidney epithelial cells) were compared using live-dead cell assay. Interestingly, results showed that **22** induced more cell death in Reh than 293T cells in both 24 and 48 h time points (Fig. S1E and F). Trypan blue assay further confirmed the above observation (data not shown). Thus our results suggest that the cytotoxic effect of **22** is less in normal cells compared to that in cancerous cells.

Since compound **22** inhibited the cell proliferation, we performed Fluorescence-Activated Cell Sorting (FACS) analysis to determine its effect on cell cycle progression. Reh and Nalm6 cells were harvested after 48 h of treatment with **22** (0.1, 0.5, 1, 5 μM), stained with propidium iodide and subjected to FACS analysis. Histogram of vehicle control showed a standard cell cycle pattern, which includes M1 (G1) and M2 (G2) separated by M3 (S) phase. The M4 (Sub G1) phase (mostly dead cells) was not prominent. Upon addition of compound, a concentration dependent change was observed in the cell cycle pattern. Most of the cells were accumulated in subG1, while number of cells in G2/M, G1 and S phases were reduced indicating cell death in presence of **22** (Fig. 1A–C). The results were comparable in both the cell lines used. However, there was no evidence for cell cycle arrest. Hence, these results further confirm that **22** induce cytotoxicity in leukemic cells, without leading to a cell cycle arrest.

The induction of apoptosis was further studied and quantified by performing annexin V-FITC/PI double-staining. Reh cells were harvested after treatment with **22** (1 μM for 48 h) were then double stained and subjected for flowcytometric analysis. Dot plot results showed that at 1 μM, 43.03% of cells were in early apoptotic stage (stained only by annexin V-FITC), while 51% were in late apoptotic stage, which was 10 fold higher than the control (Fig. 2A and B). Comparable results were obtained when the experiment was repeated. These results showed that **22** induce translocation of phosphatidyl serine leading to apoptosis.

Mitochondrial membrane potential plays an important role in induction of apoptosis. Apoptosis results in the loss of potential

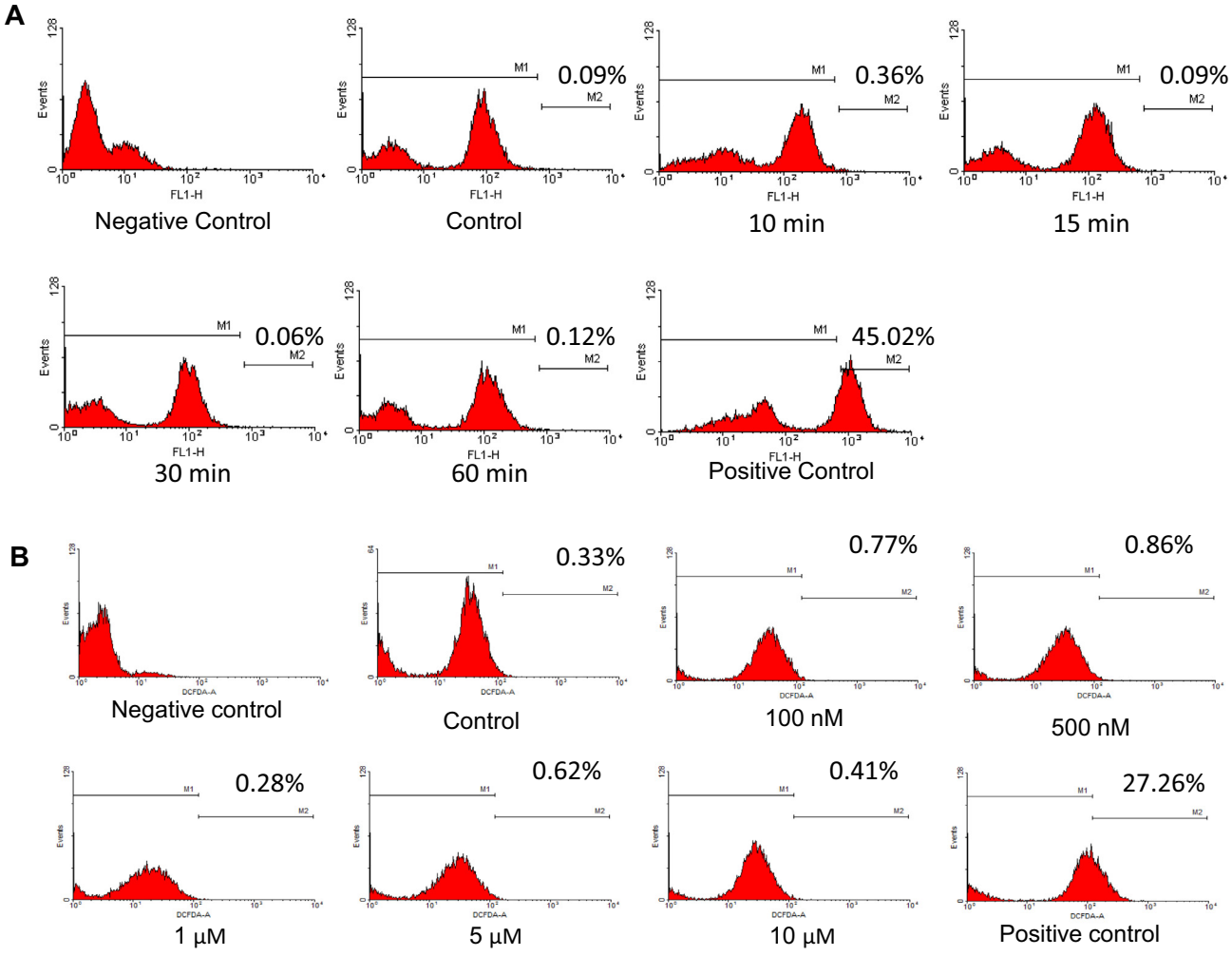

Figure 4. Determination of intracellular ROS production in Reh cells following treatment with **22**. (A) Reh cells treated with **22** (1 μM) for different time points were used for testing the formation of intracellular ROS by flow cytometry. (B) Reh cells were treated with **22** at different concentrations (0.1, 0.5, 1, 5 and 10 μM) for 10 min and assayed for ROS production. H_2O_2 treated cells were used as positive control. Cells alone were used as negative control.

which can be detected by staining with JC-1 dye.[28] JC-1 is a fluorescent cation that incorporates into mitochondrial membrane and form aggregates in healthy nonapoptotic cells. This aggregation changes the fluorescence properties of JC-1 dye leading to a shift from green to red fluorescence which has absorption/emission maxima of 585/590 nm. However, in apoptotic cells, the mitochondrial membrane potential collapses and the JC-1 cannot accumulate in the mitochondria and remains in the cytoplasm, resulting in a green fluorescent monomeric form which has absorption/emission maxima of 510/527 nm. Result showed that most of the DMSO treated cells exhibited red fluorescence. Interestingly **22** treated cells emitted green fluorescence in a concentration-dependent manner (from 1 μM onwards) and at 5 μM most of the cells showed green fluorescence which was similar to that of positive control 2,4-DNP. Thus, our results indicate that **22** altered mitochondrial membrane potential in a dose-dependent manner which further suggests the activation of apoptosis (Fig. 3A and B).

The over production of ROS is an indicator of cellular response leading to DNA damage and apoptosis. Since the compound **22** treatment resulted in apoptosis, we wondered whether there is ROS production in cell upon treatment with **22** in order to address this question FACS analysis was performed to examine ROS production after treating with **22** either at different time points (Fig. 4A) or at different concentrations of the compound (Fig. 4B). Result showed that there was no ROS generation in both conditions tested.

Since the above experiments suggested activation of apoptosis we were interested in studying expression of different apoptosis and DNA damage repair proteins by western blot analysis. The cell lysate was prepared from Reh cells after treating with compound **22** (0.5 μM and 1 μM) for 48 h. Western blot analysis showed that at 1 μM of **22**, KU70 is downregulated (Fig. 5). KU70 is a DNA end binding protein involved in nonhomologous end joining, one of the DNA double-strand break repair pathways. KU70 also has cytoprotective functions that suppresses apoptosis.[29] Hence the reduced expression of KU70 promotes apoptosis. Poly (ADP-ribosyl) polymerase (PARP) is a single strand break repair enzyme known to be cleaved by caspase 3 upon apoptotic activation. Immunoblotting analysis showed that cleavage of PARP in a concentration dependent manner, suggesting its activation (Fig. 5). Since we could observe PARP cleavage, we were interested in testing the activation of CASPASE 3, 9 and 8. Immunoblot analysis showed cleavage of caspase 3 in a concentration dependent manner. Besides, we also observed reduction in the expression of BID, a pro-apoptotic protein, particularly at 1 μM of compound **22** (Fig. 5). CASPASE 3 is activated in apoptotic cells both during extrinsic and intrinsic pathways. Since there was no distinct change in the expression of CASPASE 9 (involved in intrinsic pathway of apoptosis), activation of CASPASE 8 (involved in extrinsic pathway of apoptosis) was probed. Results showed cleavage of CASPASE 8 (Fig. 5) and up-regulation of another death receptor signaling protein FAS. Thus, our data suggest that compound **22** induce cell death by activating death receptor pathway of apoptosis.

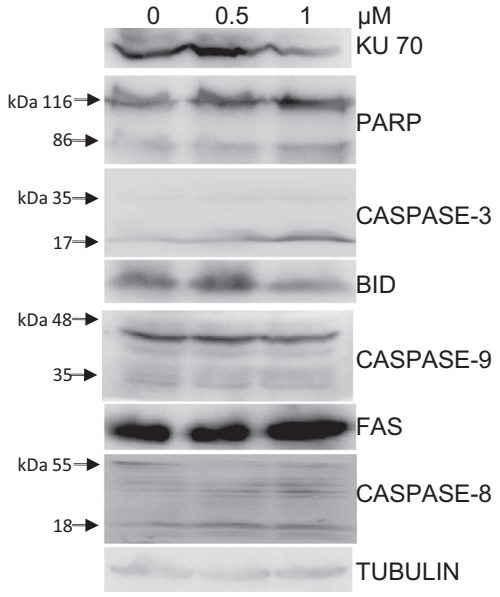

Figure 5. Expression of apoptotic proteins in Reh cells after treating with **22**. Cell lysate was prepared following treatment with **22** (500 nM and 1 μM for 48 h). DMSO treated cells were used as control. Western blotting studies were performed using specific primary antibodies against KU70, PARP1, CASPASE 3, BID, CASPASE 9, FAS and CASPASE 8. α-Tubulin was used as loading control.

In this Letter, we report the synthesis and antiproliferative activity of a series of substituted imidazo[2,1-*b*][1,3,4]thiadiazoles. Compound **22** in NCI-60 test showed a remarkable antiproliferative activity and selected for further studies. Data obtained in different leukemia cell lines revealed that compound **22** induces cytotoxicity in dose- and time-dependent manner, induces translocation of phosphatidyl serine of cells to outer membrane, and alters mitochondrial membrane potential and the expression of apoptotic and DNA-repair proteins. These results together with the activation of caspase 3 and 8 indicate that compound **22** induced cytotoxicity through extrinsic pathway of apoptosis.

Acknowledgments

We gratefully acknowledge the support for this research effort from All India Council for Technical Education (AICTE), New Delhi, India (Ref. No. 8023/BOR/RID/RPS-169/2008-09). The authors are also grateful to NMR research centre, Indian Institute of Science, Bangalore, India for recording NMR spectra for our compounds. We are grateful to the National Cancer Institute (Bethesda, MD) for the antitumor tests.

Supplementary data

Supplementary data associated with this article can be found, in the online version, at http://dx.doi.org/10.1016/j.bmcl.2014.08.032.

References and notes

1. Crawford, S. *Front. Pharmacol.* **2013**, *4*, 68.
2. Iyer, D.; Raghavan, S. C. Targeted Cancer Therapy: The Role of BCL2 Inhibitors. In *Recent Developments in Biotechnology 7 (Drug Discovery)*, 2013; Studium Press: India, pp 1–25.
3. Druker, B. J. *Adv. Cancer Res.* **2004**, *91*, 1.
4. Vogler, M.; Dinsdale, D.; Dyer, M. J. S.; Cohen, G. M. *Cell Death Differ.* **2009**, *16*, 360.
5. Srivastava, M.; Nambiar, M.; Sharma, S.; Karki, S. S.; Goldsmith, G.; Hegde, M.; Kumar, S.; Pandey, M.; Singh, R. K.; Ray, P.; Natarajan, R.; Kelkar, M.; De, A.; Choudhary, B.; Raghavan, S. C. *Cell* **2012**, *151*, 1474.
6. Gadad, A. K.; Karki, S. S.; Rajurkar, V. G.; Bhongade, B. A. *Arzneim.-Forsch./Drug Res.* **1999**, *49*, 858.
7. Terzioglu, N.; Gursoy, A. *Eur. J. Med. Chem.* **2003**, *38*, 781.
8. Kolavi, G.; Hegde, V.; Khazi, I. A.; Gadad, P. *Bioorg. Med. Chem.* **2006**, *14*, 3069.
9. Gadad, A. K.; Mahajanshetti, C. S.; Nimbalkar, S.; Raichurkar, A. *Eur. J. Med. Chem.* **2000**, *35*, 853.
10. Andotra, C. S.; Langer, T. C.; Kotha, A. *J. Ind. Chem. Soc.* **1997**, *74*, 125.
11. Khazi, I. A.; Mahajanshetti, C. S.; Gadad, A. K.; Tarnalli, A. D.; Sultanpur, C. M. *Arzneim.-Forsch./Drug Res.* **1996**, *46*, 949.
12. Andreani, A.; Leoni, A.; Locatelli, A.; Morigi, R.; Rambaldi, M.; Simon, W. A.; Senn Bilfinger, J. *Arzneim.-Forsch./Drug Res.* **2000**, *50*, 550.
13. Andreani, A.; Bonazzi, D.; Rambaldi, M.; Fabbri, G.; Rainsford, K. D. *Eur. J. Med. Chem.* **1982**, *17*, 271.
14. Andreani, A.; Rambaldi, M.; Mascellani, G.; Bossa, R.; Galatulas, I. *Eur. J. Med. Chem.* **1986**, *21*, 451.
15. Andreani, A.; Rambaldi, M.; Mascellani, G.; Rugarli, P. *Eur. J. Med. Chem.* **1987**, *22*, 19.

16. Andreani, A.; Rambaldi, M.; Locatelli, A.; Andreani, F. *Collect. Czech. Chem. Commun.* **1991**, *56*, 2436.
17. Karki, S. S.; Panjamurthy, K.; Kumar, S.; Nambiar, M.; Ramareddy, S. A.; Chiruvella, K. K.; Raghavan, S. C. *Eur. J. Med. Chem.* **2011**, *46*, 2109.
18. Hetzheim, A.; Pusch, H.; Beyer, H. *Chem. Ber.* **1970**, *103*, 3533.
19. Dhepe, S.; Kumar, S.; Vinayakumar, R.; Ramareddy, S. A.; Karki, S. S. *Med. Chem. Res.* **2012**, *21*, 1550.
20. Begum, N. S.; Vasundhara, D. E.; Kolavi, G. D.; Khazi, I. M. *Acta Crystallogr.* **2007**, *E63*, 1955.
21. Spillane, W. J.; Kelly, L. M.; Feeney, B. G.; Drew, M. G. B.; Hattotuwagama, C. K. *Arkivoc* **2003**, *7*, 297.
22. Lynch, D. E.; Ewington, J. *Acta Crystallogr., C* **2001**, *57*, 1032.
23. Isoda, S.; Aibara, S.; Miwa, T.; Fujiwara, H.; Yokohama, S.; Matsumoto, H. *Eur. Pat. Appl.* EP 279,298 A1 19,880,824, 1988.
24. Meyer, H.; Horstmann, H.; Moeller, E.; Garthoff, B. Ger. Offen. DE 3,020,421 A1 19,811,210, 1981.
25. Shichiri, M.; Tanaka, Y. *Cell Cycle* **2010**, *9*, 64.
26. Hollingshead, M.; Alley, M. C.; Camalier, R. F.; Abbott, B. J.; Mayo, J. G.; Malspeis, L.; Grever, M. R. *Life Sci.* **1995**, *57*, 131.
27. Hegde, M.; Karki, S. S.; Thomas, E.; Kumar, S.; Panjamurthy, K.; Ranganatha, S. R.; Rangappa, K. S.; Choudhary, B.; Raghavan, S. C. *Plos One* **2012**, *7*, e43632.
28. Chiruvella, K. K.; Kari, V.; Choudhary, B.; Nambiar, M.; Ghanta, R. G.; Raghavan, S. C. *FEBS Lett.* **2008**, *582*, 4066.
29. Rashmi, R.; Kumar, S.; Karunagaran, D. *Carcinogenesis* **2004**, *25*, 1867.